the dopant concentration profile is not characteristic of Fickian or case II diffusion. Rather, it is characteristic of simultaneous diffusion and rapid chemical reaction of AsF_5. In PPV doped for 5–10 days a region of nearly constant As concentration is observed just below the surface oxide layer. The relative amounts of arsenic and carbon suggest one dopant anion for every four to five PPV repeat units. When the measured doped layer thicknesses are used, the lower limit to the intrinsic electrical conductivity of AsF_5-doped PPV is estimated to be $\approx 4 \times 10^4$ $(\Omega\ cm)^{-1}$.

Acknowledgment. M.A.M. acknowledges supplemental fellowship support from the Plastics Institute of America. R.J.C. acknowledges support from the NSF/DMR Polymers Program. The use of the facilities of the Cornell Material Science Center made these experiments possible. We thank Nicholas Szabos for technical assistance. Also, we thank Professor R. S. Stein for his support. This work was supported by AFOSR Grant 88-011.

References and Notes

(1) Pekker, S.; Janossy, A. *Handbook of Conducting Polymers*; Skotheim, T. A., Ed.; Marcel Dekker: New York, 1986; p 45.
(2) Chien, J. C. W. *Polyacetylene: Chemistry, Physics, and Materials Science*; Academic Press: New York, 1984;f p 325.
(3) Dresselhaus, M. S.; Wasserman, B.; Wnek, G. E. *Mater. Res. Soc. Symp. Proc.* **1984**, *27*, 413.
(4) Crank, J.; Park, G. S. *Trans. Faraday Soc.* **1951**, *82*, 1072.
(5) Long, F. A.; Richmond, D. *J. Am. Chem. Soc.* **1960**, *82*, 513.
(6) Thomas, N. L.; Windle, A. H. *Polymer* **1977**, *18*, 1195.
(7) Mills, P. J.; Palmstrom, C. J.; Kramer, E. J. *J. Mater. Sci.* **1986**, *21*, 1479.
(8) Kanicki, J. *Handbook of Conducting Polymers*; Skotheim, T. A., Ed.; Marcel Dekker: New York, 1986; p 543.
(9) Burroughes, J. H.; Jones, C. A.; Friend, R. H. *Nature* **1988**, *335*, 137.
(10) Meijer, E. W.; Nijhuis, S.; van Vroonhoven, F. C. B. M. *J. Am. Chem. Soc.* **1988**, *110*, 7209.
(11) Foot, P. J. S.; Mohammed, F.; Calvert, P. D.; Billingham, N. C. *J. Phys. D: Appl. Phys.* **1987**, *20*, 1354.
(12) Benoit, C.; Rolland, M.; Aldissi, M.; Rossi, A.; Cadene, M.; Bernier, P. *Phys. Status Solidi A* **1981**, *68*, 209.
(13) Gagnon, D. R.; Capistran, J. D.; Karasz, F. E.; Lenz, R. W.; Antoun, S. *Polymer* **1987**, *28*, 567.
(14) Bradley, D. D. C.; Friend, R. H.; Lindenberger, H.; Roth, S. *Polymer* **1986**, *27*, 1709.
(15) Masse, M. A.; Martin, D. C.; Petermann, J. H.; Thomas, E. L.; Karasz, F. E. *J. Mater. Sci.* **1990**, *25*, 311.
(16) Masse, M. A.; Schlenoff, J. B.; Karasz, F. E.; Thomas, E. L. *J. Polym. Sci., Polym. Phys.* **1989**, *27*, 2045.
(17) Lenz, R. W.; Han, C. C.; Stenger-Smith, J.; Karasz, F. E. *J. Polym. Sci., Polym. Chem.* **1988**, *26*, 3241.
(18) Machado, J. M.; Karasz, F. E.; Kovar, R. F.; Burnett, J. M.; Druy, M. A. *New Polym. Mater.* **1989**, *1*, 189.
(19) Bradley, D. D. C.; Evans, G. P.; Friend, R. H. *Synth. Met.* **1987**, *17*, 651.
(20) Masse, M. A.; Hirsch, J. A.; White, V. A.; Karasz, F. E. *New Polym. Mater.*, in press.
(21) Chu, W.-K.; Mayer, J. W.; Nicolet, M.-A. *Backscattering Spectrometry*; Academic Press: New York, 1978.
(22) Doolittle, L. R. *Nucl. Instrum. Methods Phys. Res.* **1985**, *B9*, 344.
(23) Masse, M. A. Ph.D. Dissertation, University of Massachusetts, 1989.
(24) Crank, J. *The Mathematics of Diffusion*, 2nd ed.; Oxford University Press: Oxford, 1975.
(25) Obrzut, J.; Karasz, F. E. *J. Chem. Phys.* **1987**, *87*, 6178.
(26) Frommer, J. E.; Elsenbaumer, R. L.; Eckhardt, H.; Chance, R. R. *J. Polym. Sci., Polym. Lett.* **1983**, *21*, 39.
(27) Basescu, N.; Liu, Z.-X.; Moses, D.; Heeger, A. J.; Naarmann, H.; Theophilou, N. *Nature* **1987**, *327*, 403.

Determination of the Fold Surface Free Energy and the Equilibrium Melting Temperature for α-Phase Poly(pivalolactone) Crystals

Hervé Marand*,† and John D. Hoffman*

Michigan Molecular Institute, 1910 West St. Andrews Road, Midland, Michigan 48640

Received October 23, 1989; Revised Manuscript Received February 6, 1990

ABSTRACT: Small-angle X-ray scattering and differential scanning calorimetry were used to determine the long spacings and melting temperature of poly(pivalolactone) samples crystallized isothermally from the melt at growth temperatures in the range 190–210 °C, which spans regimes II and III. Low-angle X-ray spacings and degree of crystallinity data obtained by differential scanning calorimetry were combined to yield accurate values of l, the true crystal core thickness (i.e., the crystal stem length). The use of various heating rates to measure the observed melting temperature allowed the effect of thickening processes to be minimized. Melting temperature and lamellar thickness data were analyzed with the Gibbs–Thomson–Tammann equation to yield the equilibrium melting temperature, $T_m^\circ = 269 \pm 2$ °C, and the fold surface free energy, $\sigma_e = 61 \pm 5$ erg·cm^{-2}.

I. Introduction

Our objective is to provide a careful determination of the equilibrium melting temperature, T_m°, and the fold surface free energy, σ_e, for α-phase poly(pivalolactone) crystals as formed from the subcooled melt. Specifically, we will pay a great deal of attention to the effects of thickening on both the melting point determination and the evaluation of σ_e. The results of such an analysis can then be combined with spherulitic growth rate data to provide an accurate determination of the lateral surface

† Present address: Virginia Polytechnic Institute and State University, Chemistry Department, Blacksburg, VA 24061.

0024-9297/90/2223-3682$02.50/0

free energy, σ, and the Thomas–Staveley constant, α. In the past, most assessments[1-8] of the surface free energies, σ and σ_e, have relied on the use of the modified Thomas–Staveley equation,[9,10] where the value $\alpha = 0.1$, derived for poly(ethylene), was assumed to be universal. This expression is

$$\sigma = \alpha \Delta h_f^\circ / (A_0)^{1/2} \quad (1)$$

where Δh_f° and A_0 are, respectively, the enthalpy of fusion per unit volume and the cross-sectional area of a chain in the crystal. The results of the present study when combined with growth rate data allowed us to demonstrate that the Thomas–Staveley constant is not at all universal and strongly depends on the chemical nature of the polymer of interest; polymers where α can be determined appear to fall into two classes.[11]

Poly(pivalolactone), PPVL, is a high crystallinity, high melting point, stiff material that belongs to the general class of aliphatic polyesters.[12] Previous studies of PPVL concentrated on the crystal structure of its various crystalline modifications,[12-18] on the various chain conformations in the solid state,[15-21] and on the study of its various phase transitions.[16,22-27] PPVL is now known to exhibit three crystal forms, α, β, and γ. The α phase is obtained as the dominant phase by crystallization from the melt at temperatures above 180 °C.[15,22,23] Crystallization at larger undercoolings results in the formation of a mixture of spherulites whose crystals belong, respectively, to the α and γ phases.[15,23] In a study of the annealing of ultraquenched glasses above T_g, Pratt and Geil[25] showed that cold crystallization also results in the formation of α-phase crystals. In the same study, they determined that the lower glass transition temperature, T_g(L), of PPVL is located at 270 K. The β crystalline phase has only been obtained, so far, by cold drawing of α- and/or γ-phase material.[16,24] A similar α- to β-crystal structure change resulting from cold drawing is exhibited by polyesters based on the general formula $(CH_2CR_1R_2COO)_n$, where chain conformations in the α- and β-phase crystals are, respectively, a 2_1 helix and a planar zigzag.[27,28] (The α phases are in general lamellar chain folded systems, and the β forms are evidently fibrous.) DSC studies of the crystallization and melting behavior of PPVL were carried out by Prud'homme et al.[23] and Borri et al.[22] The former investigated the multiple melting behavior of melt-crystallized PPVL under slow cooling conditions and inferred the existence of two different crystal forms (α and γ). The latter group studied the overall crystallization kinetics by using the Avrami analysis and reported various thermodynamic and kinetic parameters of the crystallization and fusion behavior of PPVL. Noah et al.[23b] also estimated the equilibrium melting temperature of PPVL ($T_m^\circ \sim 268$ °C) and the fold surface free energy ($\sigma_e \sim 43$ erg·cm^{-2}). These values were obtained without accounting for lamellar thickening effects that may take place when melting temperatures are recorded at a low heating rate (10 °C/min).

Recently, Roitman et al.[11] examined in detail the crystal growth behavior and morphology of melt-crystallized PPVL under isothermal conditions. By analysis of the temperature dependence of the α-phase crystal growth rate, using the Lauritzen–Hoffman (LH) theory,[9] it was found that PPVL exhibits a regime II → III transition.[29] This kinetic transition occurs near 203 °C and is paralleled by a gradual morphological transition from spherulites to axialites as the temperature is increased. Another important result of this study was the discovery that the Thomas–Staveley constant,[9,10] α, for poly(pivalolactone) markedly differed from the commonly quoted value of 0.1 for other polymers. In the latter investigation the determination of the nucleation constants relied on the knowledge of both the equilibrium melting temperature and the fold surface free energy, which will be determined here.

Gibbs–Thomson–Tammann Treatment.[9,30,31] The Gibbs–Thomson–Tammann equation is generally used to quantify the melting point depression exhibited by thin platelike crystals. This expression is given by

$$T_m' = T_m^\circ (1 - 2\sigma_e / \Delta h_f^\circ l) \quad (2)$$

Here T_m' is the observed melting point for a thin platelike crystal of thickness l. The determination of T_m° and σ_e is then carried out by evaluation of the slope and intercept of the T_m' vs $1/l$ plot. Such a plot is constructed by measuring lamellar thickness and melting temperature of crystals formed at various undercoolings. However, several precautions must be observed to ensure proper use of this treatment. First, one must verify that the thin platelike crystal approximation is valid for the material investigated. Meille et al. investigated the morphology of melt- and solution-crystallized PPVL by transmission electron microscopy[15] and showed that such an approximation is indeed justified. Second, the melting temperature, T_m', must be measured under conditions where one is reasonably certain of the lamellar thickness, l, at the melting point. In the customary experiment, l is measured at room temperature and then the sample is heated to find the melting point. It is, however, well-known that polymer crystals may undergo thickening during the heating required to measure their melting temperature. To ensure that l and T_m' correspond to the same crystal thickness, the melting behavior must be followed with heating rates large enough to prohibit extensive thickening. However, when large heating rates are used in differential scanning calorimetry, attention must be paid to thermal lags.[32] The latter point can be carefully monitored if the various samples investigated have identical shape and weight.

II. Experimental Section

Poly(pivalolactone) synthesized at Tennessee Eastman Co. was kindly supplied by Prof. P. H. Geil. Although the molecular weight of this material has not been measured, we can infer from recent growth rate studies[33] that M_v must be around 250 000. PPVL samples for small-angle X-ray and differential scanning calorimetry analysis were prepared in the shape of 0.8-mm-thick rectangular slabs molded at 250 °C under 200 psi for 5 min. These samples were then crystallized isothermally in a Mettler FP2 hot stage at temperatures, T_x, ranging from 190 to 210 °C after residing in the melt state for 5 min at 260 °C. After crystallization at T_x for a specified time, the samples were quenched in iced water.

The small-angle X-ray scattering profile of these samples was obtained at room temperature with a Kratky camera using Cu Kα X-ray radiation ($\lambda = 1.542$ Å). The scattered radiation was recorded with a proportional counter by scanning the detector from $q = 0.006$ to 0.5 Å^{-1} (q is the scattering vector, $q = 4\pi \sin(2\theta)/\lambda$, and 2θ is the scattering angle). Plots of the Lorentz-corrected desmeared absolute intensities versus scattering vector, q, were obtained by correcting the raw data for parasitic air and slit scattering (background subtraction), calibrating the SAXS intensity with a primary lupolen standard, and multiplying the SAXS intensity by q^2 ("Lorentz" correction) after desmearing.[34]

Different scanning calorimetry melting studies were carried out on a Du Pont DSC Model 1090 under nitrogen flow with heating rates, R, of 10, 20, 40, 60, and 80 °C/min. The samples for these studies were cut to identical shape and weight (7.0 ± 0.2 mg) using a cork borer. The enthalpies of fusion and melting temperatures were calibrated with indium and tin standards at 1 °C/min. The melting temperatures are reported at the peak of the melting endotherm.

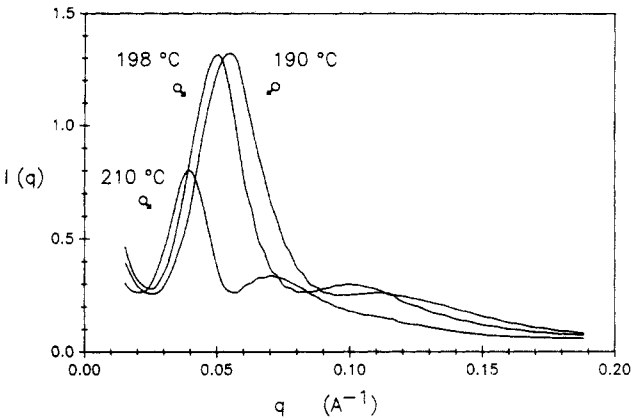

Figure 1. Desmeared Lorentz-corrected small-angle X-ray scattering profiles of samples isothermally crystallized at 190, 198, and 210 °C. SAXS profiles for other temperatures of crystallization are omitted for clarity.

Table I
Long Spacing and Lamellar Thickness as a Function of Crystallization Temperature

T_x, °C	L, Å	l,[a] Å
190	113	79
192	115	82
194	119	85
196	121	88
198	123	90
200	130	96
202	133	101
206	143	110
210	159	131

[a] Calculated by using values of ϕ_{cv} from Table II.

III. Results and Discussion

Desmeared small-angle X-ray scattering profiles of samples crystallized isothermally at selected temperatures between 190 and 210 °C are shown in Figure 1. The observed shift in the first-order maximum toward smaller angles with increase in crystallization temperature confirms the generally expected increase in long spacing with decreasing undercooling. The profiles clearly exhibit a second-order maximum that increases in sharpness with increasing crystallization temperature. This suggests a reduction in disorder of the lamellar stacking when the crystallization takes place more slowly (i.e., at low undercooling). The ratio of the angular positions of the second and first scattering maxima is relatively close to 2.00 for all temperatures of crystallization. Crist et al.[35] demonstrated that, in such conditions, it is well justified to use the first scattering maximum to calculate the average structural period of the lattice (long spacing). Long spacings, L, are then given by the Bragg relation and are shown in Table I.

$$L = 2\pi/q_{\text{first order}} \tag{3}$$

Since the degree of crystallinity of PPVL is always very high[11,12,15,23] (ca. 80%), it is reasonable to assume that the amorphous component is only located between the lamellae. Under such conditions, the lamellar thickness, that is, the crystal stem length, l, is obtained from the volume percent crystallinity, ϕ_{cv} and the long spacing, L:

$$l = \phi_{cv}L \tag{4}$$

Differential scanning calorimetry results are shown in Table II. For each heating rate, R, the melting temperature increases with crystallization temperature as is expected from the Hoffman–Weeks treatment.[36] The observed heat of fusion, Δh_f, also slightly increases with crystallization temperature, thereby implying a better folding at high T_x than at low T_x. The volume percent degree of crystallinity, ϕ_{cv}, was calculated in terms of $\Delta h_f°$, Δh_f, and the amorphous and crystalline densities, respectively, ρ_a and ρ_c

$$\phi_{cv} = (\Delta h_f/\Delta h_f°)(\rho_a/\rho_c)/[1 - (1 - (\rho_a/\rho_c))(\Delta h_f/\Delta h_f°)] \tag{5}$$

in which, of course, $\Delta h_f/\Delta h_f° = \phi_{cw}$ is the crystalline weight fraction determined by DSC. The melting temperature, T_m', recorded at the different heating rates was not corrected for thermal lag. However, since the samples for DSC analysis were of identical weight and shape, the thermal lag effects should be the same for all samples and should only depend on heating rate. To calculate the equilibrium melting temperature, $T_m°$, the T_m' vs $1/l$ data was extrapolated to $1/l = 0$ for each heating rate, which gives an apparent value of $T_m°$ appropriate to each heating rate (Figure 2). Lamellar thicknesses, which were calculated with eqs 3–5, are in the range quoted in the literature.[15,23] Table III lists the apparent equilibrium melting temperatures and the slopes of the T_m' vs $1/l$ data for the various heating rates. At a rate of 10 °C/min, the value of the apparent equilibrium melting temperature is within 1° of that reported by Noah et al.[23b] The true equilibrium melting temperature, $T_m°$, is then obtained by extrapolating the apparent equilibrium melting temperatures to a heating rate of 1 °C/min for which the DSC temperature scale was calibrated (Figure 3). This extrapolation is carried out by using only the high heating rate data where thickening is expected to occur much less readily. It may be noted that in this range the apparent equilibrium melting temperature varies approximately linearly with heating rate as would be expected from a linear variation of thermal lag with heating rate. The extrapolation procedure yields a value of $T_m° = 269 \pm 2$ °C. This value of $T_m°$ is then used to calculate the fold surface free energy of PPVL for the various heating rate experiments. Since samples crystallized at various crystallization temperatures and melted at the same heating rate should exhibit a relatively constant thermal lag, the slopes of the T_m' vs $1/l$ data sets should be independent of thermal lag and are only affected by thickening during the heating run. The fold surface free energy is then obtained by multiplication of the slope of T_m' vs $1/l$ by the constant factor $\rho_c\Delta h_f°/2T_m°$ where $\Delta h_f° = 148.5$ J/g, $\rho_c = 1.23$ g/cm^3 (ref 22), and $T_m° = 542.2$ K (Table III). At the highest actual heating rates, where thickening is highly subdued, the fold surface energy reaches a value around 58 erg·cm^{-2}. Using only the 40, 60, and 80 °C/min points, we extrapolate ρ_e vs $1/R$ to infinite heating rate ($1/R = 0$) to estimate a value of 64 erg·cm^{-2} for the fold surface energy (Figure 4). The use of a linear extrapolation is empirical but provides a reasonable upper limit for the value of the fold surface energy. As the heating rate is increased, the thickening effects should be less pronounced, since thickening generally varies as the logarithm of the elapsed time. This will tend to result in a negative curvature of the σ_e vs $1/R$ curve near $1/R = 0$. Thus one recognizes 64 erg·cm^{-2} as an upper bound. We therefore quote a value for σ_e intermediate between the extrapolated and the highest measured fold surface free energy. Thus we find $\sigma_e = 61 \pm 5$ erg·cm^{-2}.

One must now ask why the value of σ_e appears to vary with heating rate R, when in all probability σ_e is a constant. Experimentally, the apparent variation of σ_e derives from the changing slopes in Figure 2. While not quantitative, the basic explanation is straightforward. We take the slope of the $R = 80$ °C/min data (top line in Figure 2) to have

Table II
Observed Melting Temperature, Heat of Fusion, and Volume Percent Degree of Crystallinity as a Function of Crystallization Temperature and Heating Rate

	T_m', °C						
T_x, °C	10 °C/min	20 °C/min	40 °C/min	60 °C/min	80 °C/min	Δh_f,[a] J·g^{-1}	ϕ_{cv},[b] %
190	240.0	242.0	245.6	251.0	255.0	107.6	70.2
192	241.1	242.3	247.0	252.9	256.8	109.0	71.2
194	241.4	243.5	249.7	253.5	258.6	109.2	71.3
196	242.1	244.4	249.8	254.2	259.0	111.0	72.6
198	242.8	245.5	250.4	256.3	260.1	111.4	72.9
200	244.5	247.1	252.0	258.0	263.0	113.0	74.0
202	245.7	248.9	253.4	260.0	264.0	115.6	75.9
206	248.6	251.4	257.0	263.0	267.5	117.4	76.9
210	251.4	255.2	261.1	266.8	272.4	124.4	82.2

[a] The quoted values correspond to the average for samples melted at 20, 40, 60, and 80 °C/min. [b] Obtained by using ρ_c = 1.23 g·cm^{-3}, ρ_a = 1.10 g·cm^{-3}, and $\Delta h_f°$ = 148.5 J·g^{-1} from ref 22.

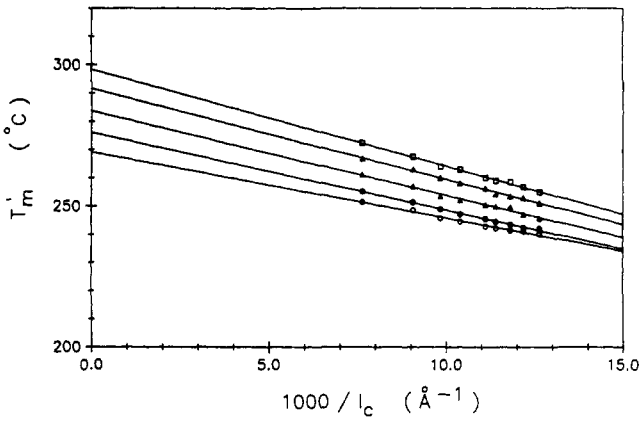

Figure 2. Observed melting temperature as a function of reciprocal lamellar thickness for heating rates of 10 (○), 20 (●), 40 (△), 60 (▲), and 80 (□) °C/min.

Table III
Extrapolated Apparent Equilibrium Melting Temperature and Fold Surface Free Energy as a Function of Heating Rate

heating rate, °C/min	$T_m°$, °C	slope T_m' vs $1/l$, 10^{-3} °C Å	σ_e, erg·cm^{-2}
10	269.1[a]	−2.34[a]	39.5[a]
20	276.1[a]	−2.75[a]	46.4[a]
40	283.6	−2.98	50.4
60	291.5	−3.20	54.1
80	298.3	−3.415	57.5

[a] These values are not included in the calculation of $T_m°$ and σ_e.

nearly the correct slope (hence, nearly correct σ_e) because thickening is minimal as a result of the rapid heating rate and assume that all the T_m' points are equally raised because of the large time-lag effect. The latter leads to an extrapolated value of T_m' that is well above the true $T_m°$, while affecting the slope but little. Consider now the lower line of Figure 2 corresponding to R = 10 °C/min. The time-lag effect is small, leading to lower T_m' values, but there is much more time during the heating run for thickening effects to predominate. If one now assumes that thin lamellae (large $1/l$) thicken faster in unit time than thicker ones (small $1/l$), then two results immediately follow: (1) the larger ($1/l$) will have larger upward shift of T_m' than the smaller ($1/l$), with the result that the slope is too low as seen in Figure 2; hence, σ_e is also too low; (2) the extrapolated T_m' will be too low for the R = 10 °C/min line as is evident in Figure 3. It strikes us as highly plausible that thin lamellae might thicken faster that thick ones, either because of the shorter longitudinal traverse or the shorter induction period for thinner lamellae. In briefer terms, it takes a high heating rate to subdue thickening effects and then develop the correct slope, but

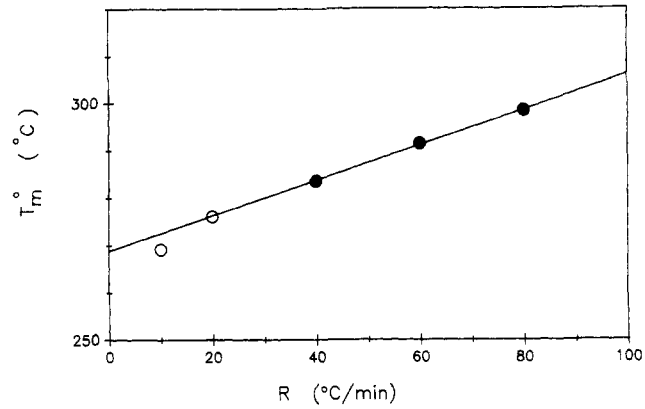

Figure 3. Extrapolated apparent equilibrium melting temperature as a function of heating rate. The low heating rate data (○) were omitted for this extrapolation since they are certainly affected by thickening processes.

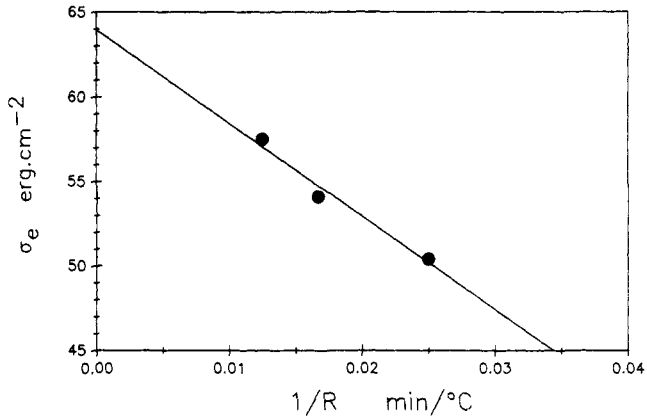

Figure 4. Fold surface free energy as a function of the reciprocal of the heating rate, R.

at the same time one incurs a large lag effect; conversely, at low heating rates there is a considerably smaller lag effect, so that one is able to detect the effect of the higher thickening rates of thin as opposed to thick lamellae, which lowers the slope and hence the apparent σ_e. Though we do not derive $1/R$ law employed in Figure 4, the foregoing provides a conceptual underpinning for omitting certain data involving low R values in Figures 3 and 4. In particular, we believe we have thereby arrived at values of $T_m°$ and σ_e that are accurate within the stated limits.

The corresponding work of chain folding is then q_f = 7.8 kcal/mol. Using the accurate value of $\sigma\sigma_e$ = 1748 erg^2·cm^{-4} previously obtained by Roitman et al.,[11] we calculate the lateral surface free energy as $\sigma = (\sigma\sigma_e)/\sigma_e$ = 29 ± 6 erg·cm^{-2}. (In earlier reports[11] we employed σ_e = 58 erg·cm^{-2} as noted above for the R = 80 °C/min run

to obtain $q_f = 7.5$ kcal·mol^{-1}.) We take the values quoted in this paper to be probably slightly more accurate; no important point hinges on these differences. It may be noted at this point that the value of σ_e measured at 10 °C/min (39.5 erg·cm^{-2}; cf. Table II) is fairly close to that reported by Noah et al.[23b] These values are, however, much lower than those calculated for higher heating rates, where we know thickening to be highly subdued. We now calculate the Thomas–Staveley constant, α, which was defined in eq 1. Using $A_o = 0.447$ nm^2, one obtains $\alpha = 0.24$. This value of α is very close to the one calculated for two other aliphatic polyesters, namely, poly(3-hydroxybutyrate) and poly(L-lactic acid), and very different from the value generally quoted for polyolefins ($\alpha = 0.1$).[37] This variation of α with the chemical nature of the polymer is not yet understood but may be related to entropic differences at the crystal/melt interface. In this regard, to gain a better understanding of the physical meaning of α, one must realize that α is defined as $\sigma/\Delta h_f^\circ A_o^{1/2}$ where σ is the isothermal work required to transport a square centimeter of segments in the crystal interior to the crystal surface and $\Delta h_f^\circ A_o^{1/2}$ is in effect the heat of fusion of a square centimeter of segments of mean thickness $A_o^{1/2}$. Thus α is the ratio of the work required to take a certain number of segments from the crystal interior to the surface to the enthalpy required to take the same number of segments from the crystal interior to the liquid state. It would be desirable to know what the enthalpic contribution of the surface free energy really is.

Using the derived value of σ_e, we can also calculate the initial lamellar thickness, l_g^*, as a function of crystallization temperature, T_x, using the Lauritzen–Hoffman kinetic theory[9]

$$l_g^* = 2\sigma_e T_m^\circ / \Delta h_f^\circ \Delta T_x + kT_x/b_o\sigma \qquad (6)$$

where ΔT_x, b_o, and k are, respectively, the undercooling, the thickness of the secondary nucleus in the growth direction, and the Boltzmann constant. With $T_m^\circ = 542.2$ K, $\Delta h_f^\circ = 182.7$ J/cm^3, and $b_o = 5.74 \times 10^{-8}$ cm, eq 7 can be written to a sufficient approximation as

$$l_g^*\ (\text{Å}) = 3620.6/\Delta T_x + 8.294 \times 10^{-3} T_x \qquad (7)$$

for $\sigma_e = 61$ erg·cm^{-2} and $\sigma = 29$ erg·cm^{-2}. For each temperature of crystallization, it is then possible to calculate the isothermal thickening coefficient, γ, defined[9] by $\gamma = l_{obs}/l_g^*$. Figure 5 describes the variations of initial lamellar thickness and thickening coefficient with crystallization temperature. One can readily observe that the isothermal thickening coefficients increase with crystallization temperature. The increase in γ with T_x is larger for higher crystallization temperatures (regime II vs regime III). This is certainly largely a consequence of the kinetics of the thickening process. It is well-known from the early work of Fischer and Schmidt[38] and Weeks[39] that thickening has a positive temperature coefficient. (Both of the papers just noted show that the lamellar thickness increases as ln t where t is the elapsed time.) It is also possible that the better chain-folding at higher temperature in regime II as compared to that at low temperature in regime III[11] may facilitate thickening in regime II. Observe that at high temperature, γ is close to 2, which is characteristic of poly(ethylene) in regime II.[9] A direct consequence of the temperature and time dependences of the thickening coefficients is the prediction that the equilibrium melting temperature of PPVL cannot readily be determined by the classical Hoffman–Weeks T_m' vs T_x method; this issue will be the subject of a forthcoming publication.[40]

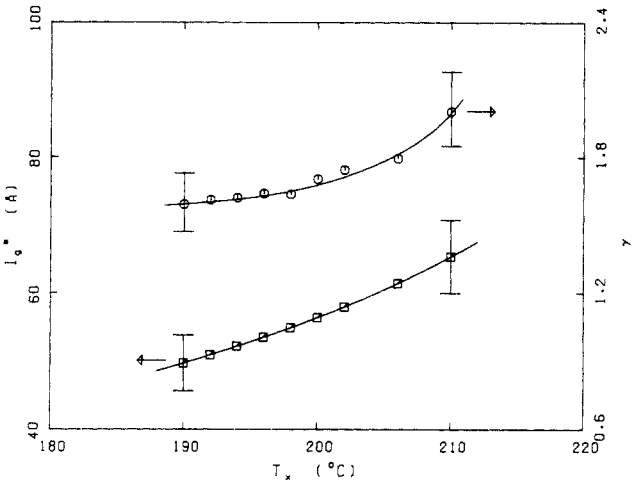

Figure 5. Initial lamellar thickness, l_g^*, and isothermal thickening coefficient, γ, as a function of crystallization temperature. The error bar is obtained by calculating l_g^* for the upper and lower bounds of σ and σ_e. Regime III applies below $T_x = 203$ °C, and regime II applies above this temperature.[11]

IV. Conclusions

Small-angle X-ray scattering and differential scanning calorimetry were used to characterize, respectively, the lamellar thickness and the melting behavior of isothermally crystallized poly(pivalolactone). The combination of a heating rate study of the dependence of the melting temperature with the classical Gibbs–Thomson–Tammann treatment allowed close estimates of the equilibrium melting temperature, T_m° (269 ± 2 °C), and the fold surface free energy, σ_e (61 ± 5 erg·cm^{-2}), to be obtained. Combined with earlier work giving $\sigma\sigma_e = 1748$ erg^2·cm^{-4}, σ was found to be 29 ± 6 erg·cm^{-2} and α came to 0.24.

Acknowledgment. We express our sincere appreciation to Dr. R. L. Miller for many fruitful discussions and for a critical review of this manuscript. We also thank Dr. J. Barnes and Dr. R. L. Briber of the NIST for their help on time-resolved SAXS experiments (not discussed here) that conclusively showed the presence of thickening processes during heating of PPVL samples above their crystallization temperature. This research was supported in part by Grant DMR 86-07707, Polymers Program, Division of Materials Research, National Science Foundation.

References and Notes

(1) Baer, E.; Carter, D. R. *J. Appl. Phys.* **1964**, *35*, 1895.
(2) Pelzbauer, Z.; Galeski, A. *J. Polym. Sci.* **1972**, *C38*, 23.
(3) Mancarella, C.; Martuscelli, E. *Polymer* **1977**, *18*, 1240.
(4) Ong, C. J.; Price, F. P. *J. Polym. Sci., Polym. Symp.* **1978**, *63*, 59.
(5) Alamo, R.; Fatou, J. G.; Guzman, J. *Polymer* **1982**, *23*, 379.
(6) Lovinger, A. J.; Davis, D. D.; Padden, F. J., Jr. *Polymer* **1985**, *26*, 1595.
(7) Phillips, P. J.; Rensch, G. J.; Taylor, K. D. *J. Polym. Sci., Polym. Phys. Ed.* **1987**, *25*, 1725.
(8) Sanchez, A.; Marco, C.; Fatou, J. G.; Bello, A. *Makromol. Chem.* **1987**, *188*, 1205.
(9) Hoffman, J. D.; Davis, G. T.; Lauritzen, J. I. In *Treatise on Solid State Chemistry*; Hannay, N. B., Ed.; Plenum Press: New York, 1976; Vol. 3, Chapter 7.
(10) Thomas, D. G.; Staveley, L. A. K. *J. Chem. Soc.* **1952**, 4569.
(11) Roitman, D. B.; Marand, H.; Miller, R. L.; Hoffman, J. D. *J. Phys. Chem.* **1989**, *93*, 6919.
(12) Carazzolo, G. *Chim. Ind. (Milan)* **1964**, *46*, 525.
(13) Perego, G.; Melis, A.; Cesari, M. *Markomol. Chem.* **1972**, *269*, 1157.

(14) Meille, S. V.; Brückner, S.; Lando, J. B. *Polymer* **1989**, *30*, 786.
(15) Meille, S. V.; Konishi, T. Geil, P. H. *Polymer* **1984**, *25*, 773.
(16) Knoblock, F. W.; Statton, W. O. U.S. Patent 3299171, 1967.
(17) Yokouchi, M.; Chatani, Y.; Tadokoro, H.; Tan, H. *Polym. J.* **1974**, *6*, 248.
(18) Brückner, S.; Meille, S. V.; Porzio, W. *Polymer* **1988**, *29*, 1586.
(19) Cornibert, J.; Marchessault, R. H. *Macromolecules* **1974**, *7*, 541.
(20) Cornibert, J.; Hien, N. V.; Brisse, R. H.; Marchessault, R. H. *Can. J. Chem.* **1974**, *52*, 3742.
(21) Veregin, R. P.; Fyfe, C. A.; Marchessault, R. H. *Macromolecules* **1986**, *19*, 2379.
(22) Borri, C.; Brückner, S.; Crescenzi, C.; Della Fortuna, G.; Mariano, A.; Scarazzato, P. *Eur. Polym. J.* **1971**, *7*, 1515.
(23) (a) Prud'homme, R. E.; Marchessault, R. H. *Makromol. Chem.* **1974**, *175*, 2705. (b) Noah, J.; Prud'homme, R. E. *Eur. Polym. J.* **1981**, *17*, 353.
(24) Prud'homme, R. E.; Marchessault, R. H. *Macromolecules* **1974**, *7*, 541.
(25) Pratt, C. F.; Geil, P. H. *J. Macromol. Sci. Phys.* **1982**, *B21* (4), 617.
(26) Allegrezza, A. E. Ph.D. Thesis, University of Massachusetts, 1972.
(27) Cornibert, J. Thèse de Doctorat, Université de Montréal, 1972.
(28) Cornibert, J.; Marchessault, R. H. *Macromolecules* **1975**, *8*, 296.
(29) Hoffman, J. D. *Polymer* **1983**, *24*, 3.
(30) Tammann, G. *Z. Anorg. Chem.* **1920**, *110*, 166.
(31) Lauritzen, J. I., Jr.; Hoffman, J. D. *J. Res. Natl. Bur. Stand. (U.S.)* **1960**, *65A*, 73.
(32) Hellmuth, E.; Wunderlich, B. *J. Appl. Phys.* **1965**, *36*, 3039.
(33) Isothermal spherulitic growth rates for α-phase PPVL obtained from Polyscience (M_v = 250 000) differ from the growth rates measured on our PPVL[11] by less than 10%.
(34) The desmearing was conducted by the method developed by P. W. Schmidt in which the deconvolution integral is approximated by a series expansion.
(35) Crist, B.; Morosoff, N. *J. Polym. Sci., Polym. Phys. Ed.* **1973**, *11*, 1023.
(36) Hoffman, J. D.; Weeks, J. J. *J. Res. Natl. Bur. Stand. (U.S.)* **1962**, *66A*, 13.
(37) Marand, H.; Roitman, D. B.; Hoffman, J. D., to be submitted for publication. For preliminary information see ref 11.
(38) Fischer, E. W.; Schmidt, G. F. *Angew. Chem., Int. Ed. Engl.* **1962**, *9*, 488.
(39) Weeks, J. J. *J. Res. Natl. Bur. Stand. (U.S.)* **1963**, *67A*, 441.
(40) Marand, H.; Prasad, A.; Roitman, D. B.; Hoffman, J. D., to be submitted for publication.

Registry No. PPVL (homopolymer), 24969-13-9; PPVL (SRU), 26497-98-3.

Relaxations in Thermosets. 7. Dielectric Effects during the Curing and Postcuring of an Epoxide by Mixed Amines

Michel B. M. Mangion and G. P. Johari*

Department of Materials Science and Engineering, McMaster University, Hamilton, Ontario, Canada L8S 4L7

Received November 14, 1989; Revised Manuscript Received February 1, 1990

ABSTRACT: The dielectric permittivity and loss during the curing of diglycidyl ether of Bisphenol A with a 0.3:0.7 (mole:mole) mixture of diaminodiphenylmethane and diaminodiphenyl sulfone have been measured from their sol to gel to glass formation regions and the effects of physical aging on their sub-T_g relaxations investigated. The permittivity monotonically decreases with the curing, but the loss initially decreases, then increases to a peak value, and finally reaches extremely low values characteristic of a glassy state. The complex permittivity plotted in a complex plane has the shape of a skewed arc similar to that of the Cole–Cole plots, and the dielectric consequences of the chemical changes with time that occur during the cross-linking of the thermoset are phenomenologically analogous to the frequency dependence of the complex permittivity of a chemically stable amorphous solid. The time dependence of the complex permittivity follows a stretched exponential decay, $\phi(t) = \exp[-(t/\tau)^\gamma]$, where $0 < \gamma < 1$. The value of $\gamma = 0.4$ at 377 K. Amongst the two sub-T_g relaxation processes observed here, the low-temperature, or γ, process is initially most prominent, but its strength decreases on physical aging while that of the β-process increases. The strength of the β-process reaches a maximum and then decreases on further aging. The α-relaxation process increasingly separates from the sub-T_g relaxations during the curing of the thermoset, and its strength decreases. Its distribution parameter decreases from 0.60 to a limiting value of 0.40 as curing proceeds. These are discussed in terms of localized segmental motions. A concept of accumulated equivalent curing time is introduced for use in both theoretical and practical investigations of a thermoset's curing, and a method for obtaining the distribution of relaxation times from limited dielectric data is proposed. The low-temperature sub-T_g relaxation is shown to have a distribution of relaxation times which remains unchanged on curing and aging.

Introduction

During the curing process of a thermoset, the reaction of a primary amine (RNH_2) with an epoxide (R'E) first forms a secondary amine (RNHR'') which in turn reacts with another epoxy group to form a tertiary amine (RNR''_2).[1-4] For a given aromatic amine, the two reactions occur concomitantly with two distinct values of chemical rate constants,[5-8] leading to the formation of a fully connected network at the gel point. The reactions continue to occur but become diffusion-controlled when the "internal viscosity" of the gel becomes very large, and this occurrence eventually leads to vitrification or the formation of a glass. The extent of reaction at the time when the mixture becomes a glass depends on the temperature of cure, but its value is found to lie approximately between 80 and 100%.[5] If a mixture of amines is used for curing, the number of rate constants accordingly increases and the extent of reaction for a given time becomes altered.

If the thermoset thus obtained is aged, its amorphous structure relaxes toward a lower energy state as a result

0024-9297/90/2223-3687$02.50/0